

CFRP Fuselage Panels Behaviour in Compression

R. Růžek^{1,*}, M. Kadlec¹, K. Tserpes², E. Karachalios³

¹ *Aerospace Research and Test Establishment (VZLU), Beranových 130, 199 05 Prague 9 - Letňany, Czech Republic*

² *Laboratory of Technology & Strength of Materials, Department of Mechanical Engineering & Aeronautics, University of Patras, Patras 265 00, Greece*

³ *Hellenic Aerospace Industry, Research and Development Department, Schimatari 320 09, Greece*

* *ruzek@vzlu.cz*

Abstract: This paper describes compressive behaviour of a reinforced fuselage composite panel. Implementation and validation of two types of strain sensors is discussed. Fibre optic Bragg grating (FOBG) sensors and standard resistance strain gauges (SGs) are used for strain history and panel behaviour validation. The mechanical tests includes different load-scenarios – compression to failure of undamaged panel, compression to failure of impacted panel and compression to failure of impacted and fatigued panel. In all cases, the panel failed due to buckling. The measurements taken from the FOBGs captured all changes in the buckling modes of the panel. Moreover, they showed a good correlation with the measurements taken from strain gauges. These findings validate the proposed strain monitoring system.

Keywords: Composite; Stiffened Panel; Sensors; Optical Fibre; Strain Gauge.

1 Introduction

Fibre-reinforced polymer composites evoked fundamental changes in the design of large, high-performance structures in the aerospace industry. The use of carbon fibre-reinforced plastics (CFRPs) is now very widespread with high impact mainly for large airframe structures. They are comprised by almost 50 % in the new Boeing 787 Dreamliner and more than 20 % in the Airbus A380. On the other hand, CFRP together with airworthiness requirements in the field of damage tolerance require significantly higher demands for the use of non-destructive testing techniques to detect damage that could counterbalance the integrity of composite structures. In the last few years, research was devoted to the development of structural health monitoring (SHM) systems, which are one step ahead from conventional non-destructive testing systems as they offer online monitoring of the structures. Recent developments in sensors and associated technologies have enabled condition-based maintenance inspection of composite structures. There exist a variety of SHM approaches, and these are of two main types: passive and active. This paper focuses on demonstrating the monitoring buckling behaviour in compression and the potential problems involved in the interpretation of the results based on sensors embedded into the structure owing to the lost local stability.

Although major aircraft manufacturers plan to develop SHM systems and integrate them into aircrafts, particularly in composite structures to the date, SHM systems were successfully installed only in experimental applications. In most of these applications FOBG-based SHM systems were applied [1–3]. In the present work, an integrated SHM methodology for CFRP fuselage panels was designed, implemented and validated on the basis of a series of load-cases representing critical scenarios for the CFRP panel. Mechanical testing of the panels and validation of the proposed SHM system are described.

2 Panel, Test Methodology and Sensor Network Description

Three stiffened composite panels were used to evaluate the sensor behaviour. Each panel consists of the skin thickness of 2 mm, three omega (Ω)-shaped stringers, and three ribs thickness of 1.5 mm. The unidirectional

HexPly 8552 (Hexcel), thickness of the prepreg ply of 0.125 mm, was used. The outer dimensions of the panels were 1650×900 mm with stringer spacing of 330 mm. The static/fatigue compression loading scenarios were chosen. Each of the panels contains different number of defects and different level of impact damages (from flaw free to visible impact damage configuration). Both barely visible impact (BVID) and visible impact damages (VID) were applied. Manufactured reference composite stiffened panel is shown in Fig. 1.

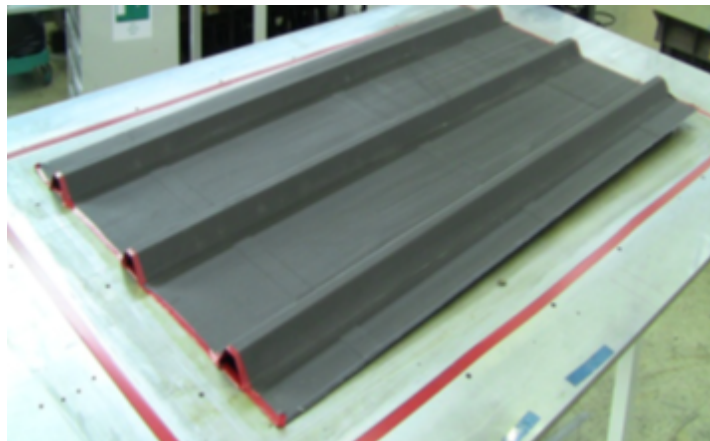


Fig. 1: Composite stiffened panel.

An FOBG sensor network was designed to enable the measurement of strains that are related to the basic damage patterns developed in the panel during loading. In each of the three panels, nine FOBGs were mounted following a configuration of three sensors per line. The sensors were bonded externally or embedded into the structure. The wavelengths of the sensors at each array were 1526 nm, 1547 nm, and 1568 nm, respectively. In the similar way, approximately seventy strain gauges (SG) were mounted on each panel. Fig. 2 shows an example of embedded FOBG routing, SG placing and damage location.

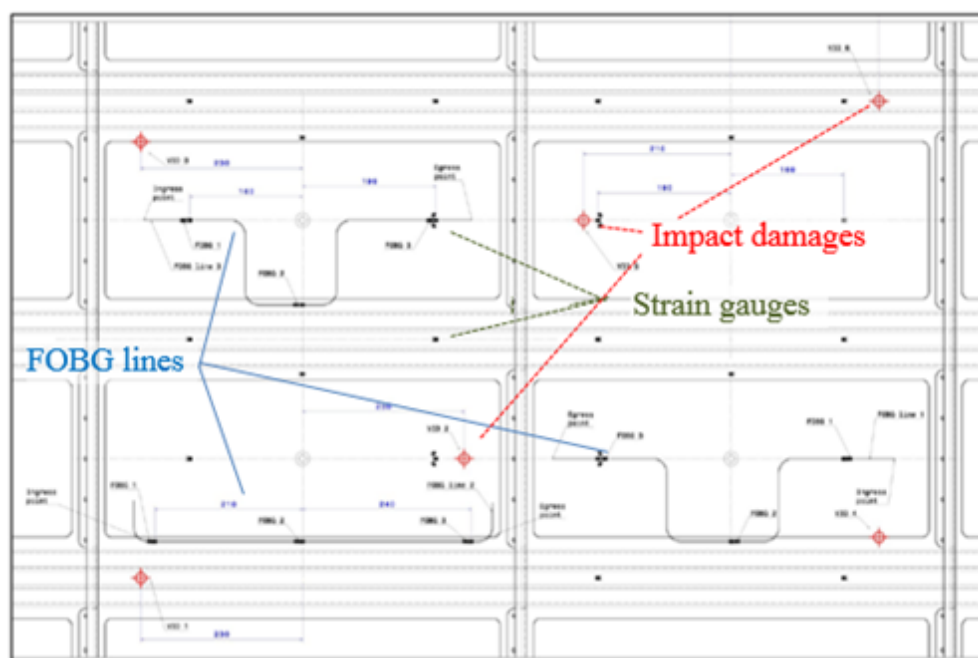


Fig. 2: Definition of FOBG sensors, strain gauges and impact damages location.

Before testing, the panels were subjected to the necessary preparation to ensure correct application of loading. To uniformly apply the boundary conditions and load and to avoid any local damage in the skin and stringers at the loaded edges, two potting frames were adjusted at the both sides of the panel. Schematic of the boundary conditions applied during the mechanical testing is shown in Fig. 3. The potting frames were made from epoxy resin which was cured inside a metallic block. Before testing, measurements were taken on the verticality of the sides of the potting frame. It was found that the two planes of the frame are not completely

vertical and the upper plane of the frame is not completely vertical to the panel and, thus, to the loading plane of the grip. This deviation possibly caused load eccentricity phenomena which should be taken into account at the evaluation of the experimental results.

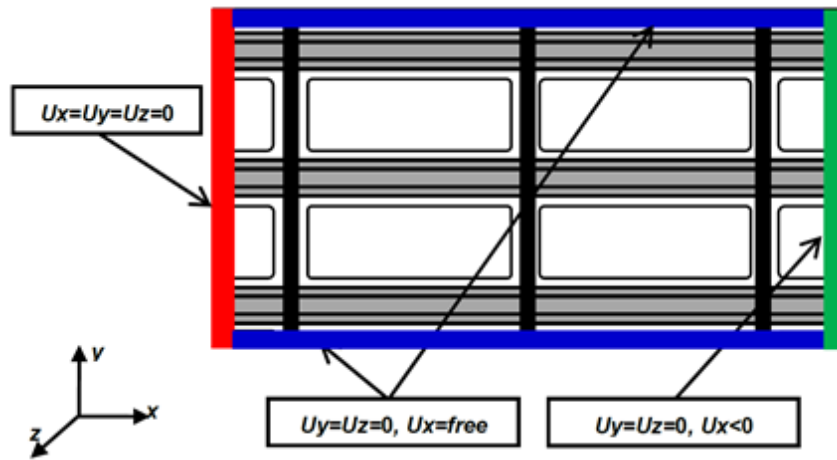


Fig. 3: Schematic of the boundary conditions applied in the model.

A standard non-destructive inspection (NDI) procedure (C-Scan) has been performed after the end of the manufacturing process for each panel so as to access the quality of manufacturing. NDI procedure was repeated after BVID and VID damages were created.

The test of the first reference panel was conducted using a quasi-static axial compression to failure. The purpose for test 1 of the reference undamaged panel was to define the reference mechanical behavior of the panel in compression. The reference panel was instrumented with axial strain gauges, rosette strain gauges and FOBG sensors bonded externally on the skin. The scope of test 2, conducted in compression with the panel in the presence of BVID and manufacturing defects, was to define static and fatigue mechanical properties. The scope of test 3, conducted in compression with panel in the presence of VID, was to determine the compressive response of the panel with VID. Both BVID and VID contained panels were instrumented with axial strain gauges, rosette strain gauges and embedded FOBGs. The displacement in compression was measured by the test machine.

All the mechanical tests were conducted using uniaxial hydraulic MTS loading machine with capacity of 1 MN. The loading rate of the reference panel was fixed to 0.25 % of the predicted ultimate load (473 kN) per second. The loading rate during quasi-static loading for the following panels was fixed to 0.25 % of the actual failure load of the reference panel. The BVID panel was subjected to compression-compression fatigue with a minimum load of -33.48 kN and a maximum load of -8.46 kN (load ratio of 0.246). The fatigue test was conducted at 4 Hz for 90,000 cycles. Afterwards, the BVID panel was subjected to quasi-static uniaxial compression to failure.

3 Results and Discussion

Fig. 4 compares the recorded load-displacement curves of the three panels loaded in compression. In all three tests, a linear relation between the applied displacement and load up to final failure was recorded. Reference panel failed at 448 kN achieved at 7.28 mm displacement. BVID panel failed at 350 kN achieved at 5.43 mm and VID panel failed at 381 kN achieved at 5.95 mm displacement. Fracture modes were very similar for all the panels. An important observation about the fracture of BVID and VID panels was that fracture of the skin and stringers seems to be related with impact damages and artificial delamination. The failure load and displacement to failure of VID panel were decreased by 15 % and 12.12 %, respectively, due to the presence of VID sites. The application of several BVID caused non-visible delamination, which either acted independently or interacted with initial artificial delamination to degrade significantly the compressive strength of BVID panel.

The accuracy of the measurements taken from FOBGs with SGs as well as their correlation with the failure sequence in the panels are crucial for the effectiveness of the proposed sensors system. The topology of the FOBG network in the panels is shown in Fig. 5. This figure documents all FOBG lines (three sensors (S) per

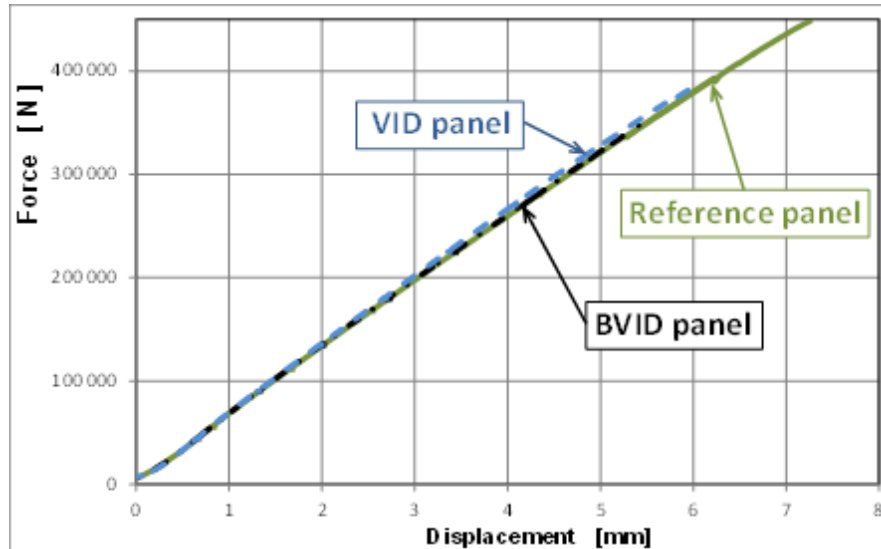


Fig. 4: Comparison of force vs. displacement curve of tested panels.

Tab. 1: Overview of panel sensor topology.

Sensor topology	1	2	3	4	5	6	7	8	9	10	11	12
Reference panel	L3S1	L3S2	L3S3	L1S1	L1S2	L1S3	L2S1	L2S2	L2S3			
BVID panel	L3S1	L3S2	L3S3	L1S1	L1S2	L1S3	L2S1	L2S2	L2S3			
VID panel	L3S1	L3S2	L3S3				L2S1	L2S2	L2S3	L1S1	L1S2	L1S3

line) in the panels. Only three lines (L) were applied to the individual panels. The lines and sensors positioning on/into the individual panels is defined in Tab. 1.

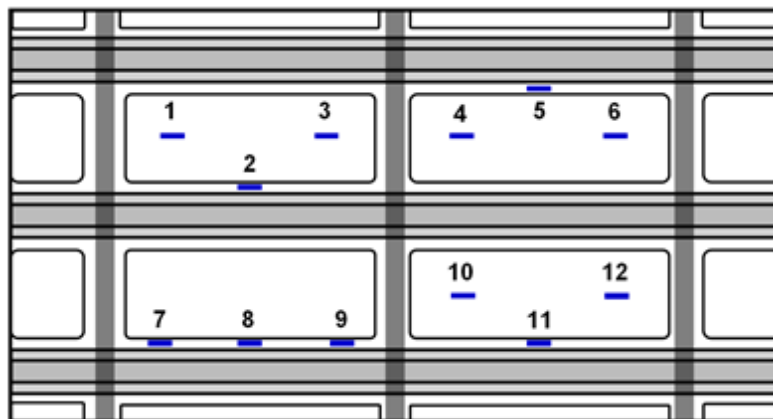


Fig. 5: Topology of sensors placed in the panels.

Fig. 6 illustrates the strain vs loading force dependences measured by the FOBGs during test of reference panel. The first local buckling occurred at skin bays at around 65 kN (14.5 % of the failure load). This local buckling was detected by L1S3 and L1S1 sensors, which are placed at the skin bay. Next buckling initiated also at the other skin bays under a little bit higher load levels as indicated by the change in the measurements of L2S1 and L2S3. The next events that indicated the changes in the buckling mode of the skin occurred at 225 kN (captured by L2S1, L2S3, L1S1, L3S2 and L2S2), at 335 kN (captured by L1S1 and L1S3), 390 kN (captured by L2S1, L3S1, L3S2 and L3S3) and 405 kN (captured by L1S2). The data measured using L2S2, L3S1, L3S2, L3S3 and L1S2 sensors are constantly compressive varying almost linearly with applied load. All these sensors are placed on the stringers. No major changes in the deformation took place in the areas around

the stringers. On the contrary, the large variation in the measurements of L1S3, L2S1, L1S1 and L2S3 sensors located in skin bays areas indicates large variation in the deformation. The plots measured for other panels show very similar behaviour.

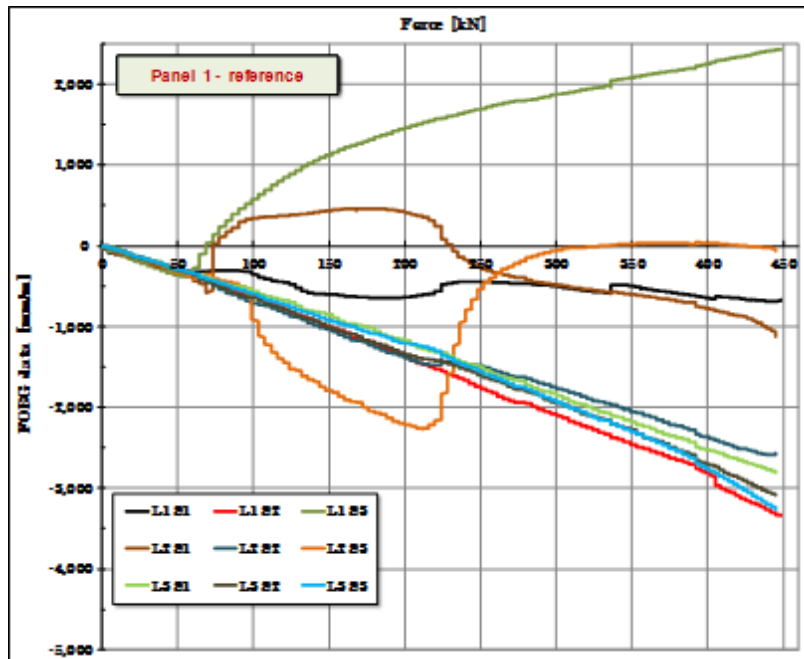


Fig. 6: FOBG strain history during static test of the reference panel.

In general, the FOBGs captured all events in the three panels which are mainly related to the change in the buckling mode of the skin. The measurements from FOBGs placed in the bay areas can be translated into useful information regarding the structural health of the panel. Regarding final failure, the FOBG measurements did not give a clear warning possibly due to the fact that final failure occurs suddenly. However, if strain to failure is known, then the strain values of the FOBGs can be the warning themselves and also give information about residual strength of the panel.

To validate strain measurements of FOBGs, the strain measurements of SGs were used. The locations of some SGs were selected to coincide with FOBGs. Fig. 7 shows comparison of the strain data of FOBGs L1S3 and L3S1 with the SGs 1113, and 1163, respectively, for reference panel. Until the first buckling in the panel structure (force lower than 65 kN), a perfect agreement between L1S3 and 1113 was achieved. For this case, the accuracy of the measurement taken by the FOBG was validated. At 65 kN, local buckling initiated at the bay where strain was measured. The measurements from the FOBG and the SG were quite similar up to 115 kN load. After that load, they deviated significantly due to the alteration of the buckling modes, which occurred in the location of the two sensors positioned in opposite panel sides. Regarding the measurements taken from L3S1 and 1E63, they coincided up to 115 kN. After that point, they started to deviate. The measurement of FOBG L3S1 seems to be not affected by the buckling while the measurement taken from 1E63 changed from negative to opposite due to buckling. The same correlation between FOBGs and SGs was observed for other panels.

4 Conclusion

In general, the comparison between FOBGs and SGs validates the accuracy of the measurements taken from FOBGs. No significant differences were found. In all cases, prior to buckling occurring, the measured strains between the sensors coincided. When buckling was started, the measurements of some sensors started to deviate mainly due to the different buckling curvature of the measurement locations. Differences were mainly observed in the case of sensors which were placed on/in the skin in areas where buckling curvature is significant. This is probably due to combination of the following facts: the SGs were placed on the surface of the skin contrary to FOBG sensors which are placed on the opposite side of the skin or were embedded into the composite structure; the significant buckling amplitude invokes the occurrence of bending loads which can result to tension strain

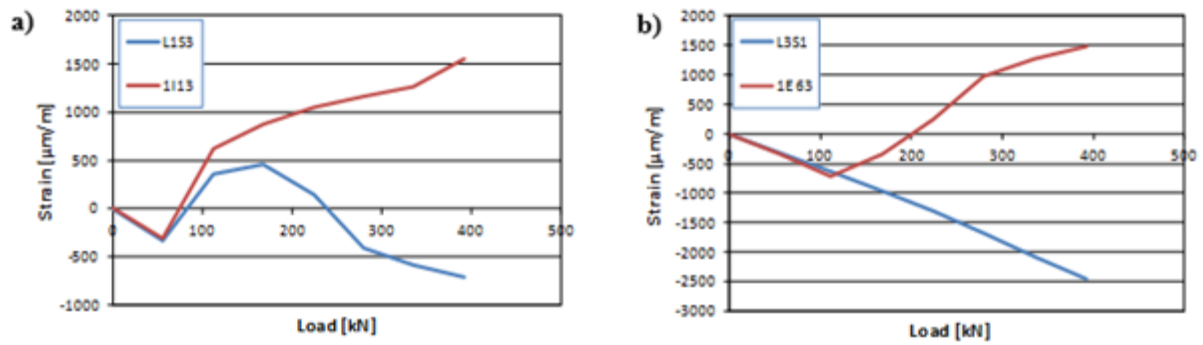


Fig. 7: FOBG strain history during static test of the reference panel.

on one skin surface and compression strain on the opposite skin surface. The above statements are verified by the fact that the agreement between FOBG and SGs data is very good for the entire loading procedure in case of sensors placed on the stringers which did not buckle.

References

- [1] Takeda S., Okabe Y., Takeda N., Delamination detection in CFRP laminates with embedded small-diameter fiber Bragg grating sensors. *Composites Part A*, 2002, 33(7), 971–80.
- [2] Baker W., McKenzie I., Jones R., Development of life extension strategies for Australian military aircraft, using structural health monitoring of composite repairs and joints. *Composite Structures* 2004, 66, 133-143.
- [3] Fu T., Liu Y., Li Q., Leng J., Fiber optic acoustic emission sensor and its applications in the structural health monitoring of CFRP materials. *Opt Lasers Eng* 2009, 47(10), 1056–62.